Nonlinear Estimation of Longitudinal Tire Slip Under Several Driving Conditions

Christopher R. Carlson
Stanford University
Mechanical Engineering
Stanford, CA 94305-4021, USA
crcarlson@stanford.edu

J. Christian Gerdes
Stanford University
Mechanical Engineering
Stanford, CA 94305-4021, USA
gerdes@cdr.stanford.edu

Abstract

This paper presents an effectively unbiased nonlinear estimation scheme which identifies tire longitudinal stiffness and effective radius using GPS and ABS wheelspeed sensors. This estimation strategy is then used to experimentally identify the longitudinal stiffness and effective radius of a summer tire and a winter tire under several different test conditions. The data clearly shows that there are several important parameters which govern tire longitudinal stiffness behavior in the low slip region. At a minimum, inflation pressure, tread depth, normal loading and temperature have a strong influence on longitudinal stiffness estimates; the change from dry to wet asphalt had the smallest effect on longitudinal stiffness estimates.

1 Introduction

Several research groups propose road friction estimation schemes under the premise that tire longitudinal stiffness for low values of slip indicates the peak value of the force slip curve [4, 8, 12, 15, 21, 23]. Such information could be valuable for applications such as driver assistance [16] and stability control systems which use force based tire models [22]. Unfortunately, the current estimation schemes in the literature return a wide range of stiffness estimates [21] for similar conditions. Typical variation ranges from 20% to 100% for individual tires on a relative scale and by up to an order of magnitude across all tires on an absolute scale. Although these schemes may be self calibrated to identify fast changes in the tire-force characteristic, it is not possible to identify slowly varying relationships such as stiffness change due to a slow inflation pressure leak or tread wear with the presented levels of variance.

The authors in [5] develop a nonlinear estimator which consistently returns true parameter estimates in simulation to within 3%. The accuracy afforded by the new estimator structure motivated the experimental characterization of the relationship between tire inflation pressure and longitudinal stiffness estimates. This current work goes on to characterize the influence of tire inflation pressure, normal load, tread depth, frictional heating and surface lubrication on longitudinal stiffness and effective radius for two different types of tires. The results show that the tire properties depend strongly upon the first four factors and weakly upon road lubrication for the levels of slip experienced under normal driving.

2 Modeling

2.1 Tire model

The SAE definition for wheel slip is:

$$\text{Slip} \quad = \quad -\left(\frac{V - R\omega}{V}\right) \tag{1}$$

Where V is the velocity of the center of the tire, R is the effective radius of the tire and ω is angular velocity of the tire. Empirical tire models, such as the Magic Formula [2], model the relationship between force transmitted by the tire and the resulting slip with complicated nonlinear relationships. Figure 1 shows typical force-slip curves of the Magic Formula for different values of road surface to tire friction. During ordinary driving, however, the tire slip rarely exceeds 2%. By linearizing the model in this small region, the force slip relation can be characterized as:

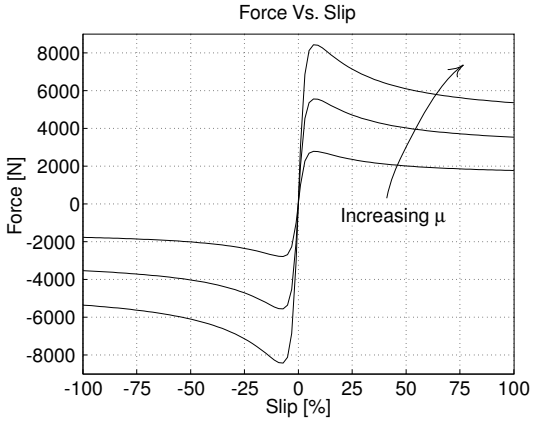

Figure 1: Magic Formula tire model curves for increasing μ

$$F \quad = \quad C_x\left(\frac{V - R\omega}{V}\right) \tag{2}$$

Where F and C_x are the force and longitudinal stiffness of the tire(s) transmitting the force.

2.2 Force Estimation

The dominant efforts acting on the tires during normal driving are illustrated in figure 2.

$$ma \quad = \quad F_x - F_{rr} - F_d - mg\sin(\theta) \tag{3}$$

Where F_x is the longitudinal force from the powertrain, F_{rr} is the rolling resistance, F_d is the aerodynamic drag and

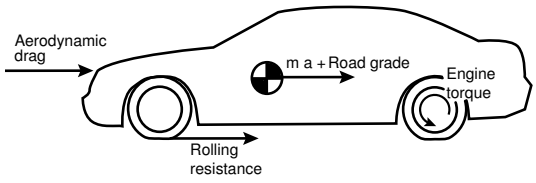

Figure 2: Force diagram for test vehicle

$mg\sin\theta$ is the contribution of road grade with angle θ. All of these terms except the powertrain may be estimated using GPS and automotive sensors [1]. However, the work appearing in this paper simplifies the force balance as much as possible. Vehicle testing is performed on flat roads to eliminate the effect of road grade. Speed is kept below $15[m/s]$ to minimize the forces due to aerodynamic drag and the engine forces are kept high with respect to the neglected terms. During these testing conditions the forces transmitted by the tires are assumed to be inertial forces and they are estimated by multiplying the vehicle mass by the acceleration at the center of gravity. Therefore only the averaged driven tire parameters are identified.

2.3 Vehicle Velocity Estimation

Until recently it has been difficult to measure absolute vehicle velocity accurately. Inertial measurement based observers were proposed in [4]. Work in [6] and [14] discuss the advantages of using Global Positioning System (GPS) velocity as an absolute velocity sensor for measuring slip. While GPS could be used directly, this paper assumes the vehicle is rear wheel drive and that the front wheels are free to roll at all times. Absolute vehicle velocity is calculated by first identifying the average of the front wheel free rolling radii to sub-millimeter accuracy using GPS; vehicle velocity is then calculated by multiplying the identified tire radii by the wheel speed measurement similar to the work in [9].

3 Linear Estimation Algorithms

3.1 Force Formulation

Previous work in [14] estimates the driven tire parameters C_x and R_d by formulating equation 2 as a linear regression:

$$\hat{a} \quad = \quad \begin{bmatrix} -\frac{1}{m} & \frac{\hat{\omega}_d}{m\hat{V}} \end{bmatrix} \begin{bmatrix} C_x \\ R_d C_x \end{bmatrix} \tag{4}$$

Where m is the mass of the vehicle and $\hat{a}, \hat{\omega}_d, \hat{V}$ represent vehicle acceleration, front wheel angular velocity and vehicle velocity. The $\hat{hat}$ notation represents measured values or values calculated from measurements.

For this investigation, vehicle velocity V is measured as:

$$V \quad = \quad R_u \dot{\theta}_u \tag{5}$$

where R_u is the undriven wheel free-rolling radius and θ_u is the average undriven wheel angular displacement measured by an ABS variable reluctance sensors. R_u is assumed constant and is estimated separately using GPS. The time derivatives of the wheel angle measurements θ_x are not directly available and are estimated as

$$\hat{\dot{\theta}}_x = \frac{\hat{\theta}_x^{k+1} - \hat{\theta}_x^{k-1}}{2T} \tag{6}$$

Where $\hat{\theta}_x$ is the measured front or rear wheel angle measurement and T is the sampling time. Likewise the acceleration is calculated by double differencing the average of the free rolling wheel angular displacement. For the remainder of this paper, the subscript u will refer to the undriven wheel and the subscript d will refer to the driven wheel.

One way to interpret this formulation is that the estimator is seeking to minimize the force error in the least squares sense, which is not the same as minimizing the measurement errors. This is well known to introduce parameter biases except for very special noise structures [13].Section 5.3 demonstrates that these biases can be quite large, even for small measurement noise values.

3.2 Linear Truth Simulation

The large biases inherent to the linear formulations are demonstrated by a continuous time simulation which models force, velocity and slip using equation 1. All other dynamics such as vehicle pitch and tire deformation are ignored. The errors of the wheel angular displacement signals are modeled as white noise which is added to the simulated sensor measurements. The standard deviations used to model the noise of the wheelspeed measurements is $0.04[rad]$ which is less than the resolution of the wheel angle sensor $[100 counts/rev]$. The simulated vehicle accelerates at $3[m/s^2]$ and decelerates at $-1[m/s^2]$ for times which yield an average velocity of $13[m/s]$. These accelerations are physically realizable by our test vehicle and were chosen to mimic accelerations and velocities during data collection conditions which appear later in this paper.

Figure 3 illustrates parameter estimation results of twenty simulated data sets. The force formulation consistently un-

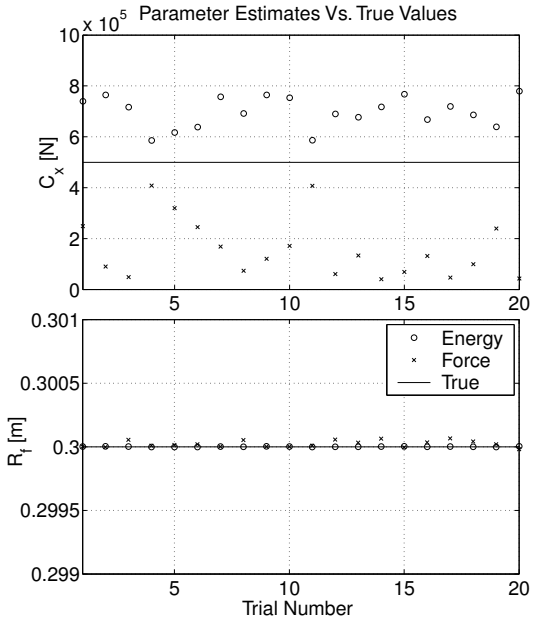

Figure 3: Truth simulation for linear parameter estimation schemes

derestimates the longitudinal stiffness by about a factor of 5, an alternate formulation in terms of energy (see [5]) tends to over estimate the stiffness by about 50%. It is interest-

ing to note that the wheel radius is consistently estimated to submillimeter accuracy by both linear estimation schemes despite the large variation in longitudinal stiffness.

If these linear schemes fail to provide reasonable parameter estimates for such idealized simulation studies, it is highly unlikely they will perform better for real data. This suggests a new approach is needed to solve this problem.

4 Nonlinear Formulation

In the spirit of a least squares solution, the optimization problems presented here seek to minimize the *measurement errors* $[\Delta\theta_d;\Delta\theta_u]$ in the driven and undriven wheel angle measurements θ_d and θ_u. The philosophy of this optimization is called, *orthogonal regression*, *errors in the variables* (EIV) or more recently a *Total Least Squares* (TLS) problem. For linear systems, this data analysis technique yields strongly consistent, asymptotically unbiased parameter estimates if the noise on the variables is independent and identically distributed (IID) with equal or known variances [11]. The problems above are posed using two identical sensors. Although these sensors are coupled through the dynamics of the vehicle, their error variances are virtually identical and in practice and simulation their errors do not appear to be correlated.

Explicitly introducing measurement noise perturbations into equation 2 and moving all terms to the right hand side yields:

$$\begin{aligned} &mR_u^2(\theta_u + \ddot{\Delta\theta_u})(\theta_u + \dot{\Delta\theta_u}) + \\ &\quad C_x\left(R_u(\theta_u + \dot{\Delta\theta_u}) - R_d(\theta_d + \dot{\Delta\theta_d})\right) = 0 \end{aligned} \tag{7}$$

The solution to these problems will be iterative and the time derivatives are approximated by first order finite difference equations. Let each measurement be written as:

$$\hat{\theta}^k = \theta^k + \Delta\theta^k$$

then,

$$\dot{\hat{\theta}}^k \cong \frac{\hat{\theta}^{k+1} - \hat{\theta}^{k-1}}{2T} \tag{8}$$

$$\ddot{\hat{\theta}}^k \cong \frac{\hat{\theta}^{k+2} - 2\hat{\theta}^k + \hat{\theta}^{k-2}}{4T^2} \tag{9}$$

where k represents the discrete time step and T represents the digital sampling rate.

The goal of minimizing the sum of the squared measurement errors, which should yield the correct parameter estimates in the presence of Independent Identically Distributed (IID) noise, can then be stated:

$$\begin{aligned} &\text{Minimize: } \|\Delta\theta_u;\Delta\theta_d\| \\ &\quad \text{Subject to: } f^k(\hat{\theta}_u,\hat{\theta}_d,\Delta\theta_u,\Delta\theta_d,R_d,C_x) = 0 \end{aligned} \tag{10}$$

Additionally, the energy formulation of the force slip equation may be similarly manipulated into this form.

Fortunately the cost function for this optimization problem is locally quasiconvex for physically meaningful parameter values as demonstrated in [5]. As such once the true values are bracketed, a bisection algorithm is guaranteed to converge to the optimal solution. The following section shows how to cast this problem as nonlinear least squares problem which converges with significantly less computational effort.

5 Nonlinear Estimation Algorithm

This section presents two improvements to the standard bisection algorithm. The first improvement is to reinterpret the problem as a nonlinear least squares problem which converges faster than the previously proposed algorithms, the second uses the sparce structure of the cost function gradient to speed up the required linear algebraic operations.

5.1 Nonlinear Total Least Squares

Bisection algorithms are guaranteed to converge for quasiconvex functions but may take many iterations to do so. A faster methodology for these problems solves the optimization problems as nonlinear total least squares (NLTLS) problems [11] with backstepping.

Let f be the true nonlinear model:

$$f(\theta_u, x) = \theta_d \tag{11}$$

where θ_u and θ_d are vectors of true model values and $x = [C_x, R_d]^T$ is the vector of model parameters. Assume that the vectors of measurements are disturbed by noise

$$\hat{\theta}_u = \theta_u + \Delta\theta_u \tag{12}$$

$$\hat{\theta}_d = \theta_d + \Delta\theta_d \tag{13}$$

Just as with ordinary least squares, if the sum of the squared measurement errors are minimized, the true parameter values will be returned. This may be written as a NLTLS problem,

$$\underset{x,\,\Delta\theta_u,\,\Delta\theta_d}{\text{Minimize:}} \quad \left\| \begin{array}{c} \Delta\theta_u \\ \Delta\theta_d \end{array} \right\| \tag{14}$$

$$\text{Subject to:} \quad f(\hat{\theta}_u - \Delta\theta_u, x) = \hat{\theta}_d - \Delta\theta_d \tag{15}$$

Problems of this form may be solved by writing an equivalent nonlinear least squares problem of higher dimension [20],

$$\underset{\theta_u,\,x}{\text{Minimize:}} \quad \left\| \begin{array}{c} f(\theta_u, x) - \hat{\theta}_d \\ \theta_u - \hat{\theta}_u \end{array} \right\| \tag{16}$$

Solutions to these problems iteratively approximate the nonlinear function as quadratic and solve a local linear least squares problem. To see this, let

$$\Theta = \left[\begin{array}{c} x \\ \theta_u \end{array} \right] \tag{17}$$

$$g(\Theta) = \left[\begin{array}{c} f(\theta_u, x) - \hat{\theta}_d \\ \theta_u - \hat{\theta}_u \end{array} \right] \tag{18}$$

Then iteratively solve the problem,

$$J^i = \left.\frac{\partial g(\Theta)}{\partial \Theta}\right|_{\Theta^i} \tag{19}$$

$$\Theta^{i+1} = \Theta^i + \alpha J^\dagger g^i(\Theta^i) \tag{20}$$

until the Θ^i converges, where i refers to the iteration number, $\dagger$ represents the least squares pseudoinverse and $0 < \alpha < 1$ is the backstepping parameter. The initial conditions may be educated guesses, for this paper the routine starts with the linear least squares parameter estimates and zeros for the measurement errors. Typically the solution converges in less than ten iterations and a backstepping parameter of $\alpha = 0.8$ works well.

5.2 Exploiting Structure

The QR factorization (QRF) is a powerful tool for finding the pseudoinverses of matrices. Algorithms for finding the QRF quickly by exploiting sparcity patterns in matrices are covered in [3, 7]. Algorithmic improvements are easily realized once the structure of the gradient matrices in equation 19 are made clear.

The gradient of Equation 11 with respect to the regressors $\Theta = [{\theta_u}^T, x^T]^T$ has the structure,

$$J = \begin{bmatrix} \frac{\partial f(\theta_u, x)}{\partial \theta_u} & \frac{\partial f(\theta_u, x)}{\partial x} \\ \frac{\partial (\theta_u - \hat{\theta}_u)}{\partial \theta_u} & \frac{\partial (\theta_u - \hat{\theta}_u)}{\partial x} \end{bmatrix} \quad (21)$$

$$= \begin{bmatrix} B_{n\times n} & D_{n\times 2} \\ I_{n\times n} & 0_{n\times 2} \end{bmatrix} \quad (22)$$

where n is the number of data points and $B_{n\times n}$ represents a banded $n \times n$ matrix and $D_{n\times 2}$ is a dense $n \times 2$ matrix. For the force formulation, equation 7, the matrix has 5 bands. Techniques outlined in [3] for solving Tikhonov regularized problems, via Givens rotations for example, are easily adapted to find the least squares inverse for matrices with this structure.

5.3 Simulation Proof of Concept

The above algorithm, run on the same truth simulation as in the linear case in figure 3, yields estimates for C_x and R_d in figure 4. The nonlinear force and energy form parameter estimates consistently estimate the longitudinal stiffness to within about 2% or 3% for data sets on the order of 600 points long.

These simulation results show that a nonlinear estimation strategy which incorporates detailed attention to the way the noise enters the force-slip model solves many of the problems encountered with the linear formulations.

6 Test Setup and Results

This section shows that the nonlinear estimation schemes defined above return extremely consistent parameter estimates from vehicle test data recorded under several driving conditions.

6.1 Test Apparatus

The experimental tests were performed on a rear wheel drive 1999 Mercedes E320 with stock installed variable reluctance Antilock Braking System (ABS) sensors. Additional equipment includes a Novatel GPS receiver and a Versalogic single board computer running the MATLAB XPC embedded realtime operating system. This system records and processes 20 data streams comfortably at sample rates up to 1000 hz.

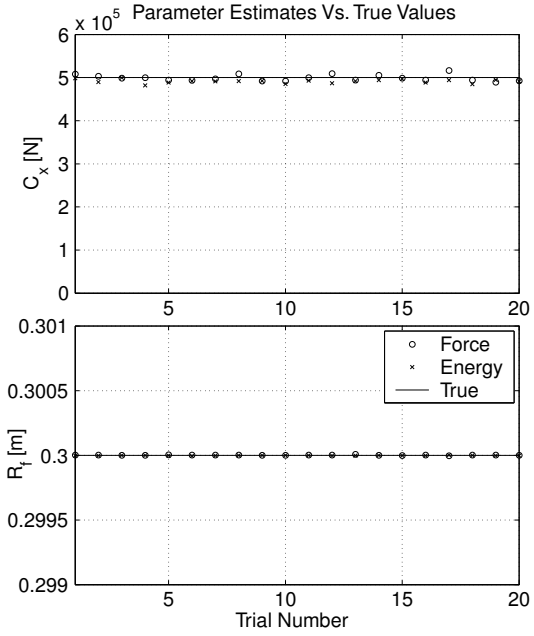

Figure 4: Truth simulation for nonlinear parameter estimation schemes

In an effort to hold as many tire variables constant as possible, the data for these results were collected on the same section of asphalt on a flat, straight, dry runway parallel to eliminate the effects of turning and road grade from the measurements. Force was applied to the tires by accelerating with throttle and decelerating with engine braking only. Thus the undriven wheels were free to roll at all times. The test road has no overhanging trees or tall buildings nearby so the GPS antenna had an unobstructed view of sky and was unlikely to experience multipath errors. Wheel angular displacements were recorded at 200Hz, summed over the length of the data set and then sub-sampled at 10Hz to reduce the auto correlation of high frequency wheel modes and reduce the computational cost of the nonlinear solution. Data sets are on the order of 600-900 points long.

6.2 Test Matrix

In an effort to identify the relative importance of inflation pressure, tread depth, vehicle loading and surface lubrication for longitudinal slip estimation, the following tires:

1. ContiWinterContact TS790, 215/55 R16
2. Goodyear Eagle F1 GS-D2, 235/45 ZR17

were tested under the conditions outlined in table 1. Testing a tread depth of $2.5[mm]$ shows the performance of a tire toward the end of its operational life.

6.3 Data Discussion

Figure 5 shows the results of several tests. Each circle represents one $45-60$ second data set during the bracketed test conditions. As such, each cluster represents a series of six data sets taken consecutively. An interesting feature of the data clusters is that they all trend down and to the

Tire Test Matrix			
#	Pressure	Tread	Weight
1	nominal	full	driver only
2	-10%	full	driver only
3	-20%	full	driver only
4	nominal	2.5[mm]	driver only
5	nominal	full	driver +200[kg]
6	nominal	full	driver +400[kg]
7	nominal	full, wet	driver only

Table 1: Test matrix for performance and winter tires

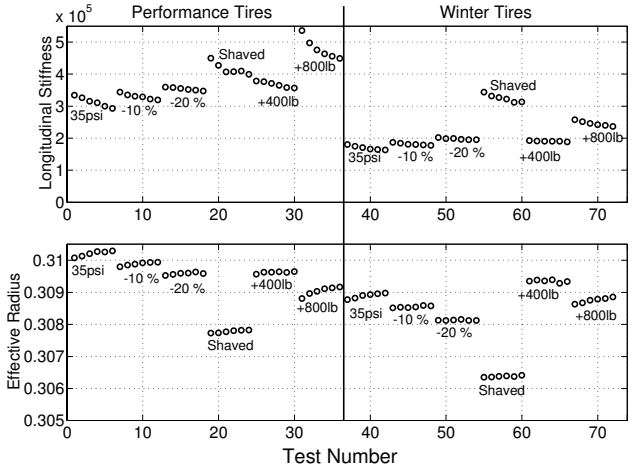

Figure 5: Tire parameters for various testing conditions

right. The process of testing the tires alters their longitudinal stiffness properties in at least two different ways. The slipping of the tire raises its internal temperature which expands the air inside the tire; typical internal pressure variation was $1-2[psi]$ pre to post data run. Additionally, the elastomeric properties of the rubber itself change. As the tire heats up, the rubber becomes easier to deform and thus lowers the tire's longitudinal stiffness. The first clusters in Figure 6 show a series of 25 data sets taken consecutively to explore this behavior. The estimates come to steady state after about 10 data runs when the frictional heating during the run equalled the cooling during the return lap to the starting point of the test. The consistency of the parameter estimates during these experiments is extremely good, within about 2.5% for longitudinal stiffness estimates, and lends credibility to the simulations performed in the previous section.

Table 2 shows the relative longitudinal stiffness change

Longitudinal Stiffness Change		
Test	Performance	Winter
Cold-hot temp	-17 %	-21 %
-10% pressure	17 %	15 %
-20% pressure	29 %	28 %
Reduced Tread	34 %	91 %
+200 [kg]	13 %	7 %
+400 [kg]	60 %	42 %
Wet Road	4 %	-2 %

Table 2: Longitudinal stiffness change from nominal

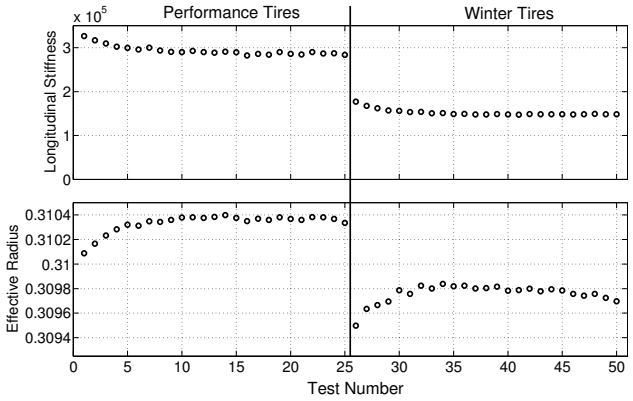

Figure 6: Convergence of tire parameters over several identical tests

from nominal for each entry of the test matrix. For the case of cold-hot, the longitudinal stiffness change due to rubber heating was isolated by subtracting the predicted longitudinal stiffness change due to the 1-2$[psi]$inflation pressure rise.

The data in Figure 7 show 8 data sets taken after a day of rain while the road is still wet and actively sprayed with fresh water. Unfortunately, the tests had to be stopped for a few minutes to refresh the water supply on every forth run, the tire cooling during the water change explains the rise in stiffness between tests 4 and 5 during the wet tests. The influence of road lubrication is clearly smaller than that of any other influence. *It is highly unlikely that an estimator could identify this surface as particularly wet during normal driving, even if all other parameters were given.*

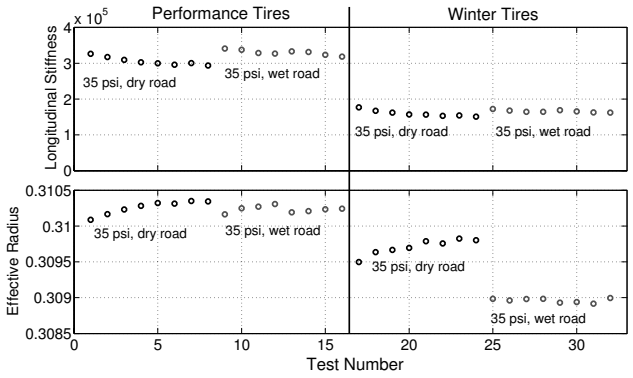

Figure 7: Comparison of tire parameters for dry verses wet asphalt

The wheel effective radius estimates are remarkably consistent, regularly returning values with submillimeter accuracy. It is interesting to note that the wheel effective radii vary by less than one millimeter for tire pressure changes of 20%.

The snow tires exhibit the most surprising wheel radius behavior, a $\frac{1}{2}$ millimeter reduction of effective radius for the snow tires on a lubricated road surface and the increase of effective radius for higher normal loading. This and the rest of the data presented in this section suggests that tires are

extremely complex and detailed care should be taken whenever inferring information solely from lumped parameters such as longitudinal stiffness and effective radius.

7 Conclusions

Although it is common practice to place measurements in the estimation matrix for linear least squares, the estimation of longitudinal stiffness and effective radius with wheel-speed sensors returns significantly biased parameter estimates. This motivated the introduction of new nonlinear estimation schemes which appear to be unbiased when the modeling assumptions hold. Using this improved estimation strategy, longitudinal stiffness and effective radius of two different kinds of tires were carefully tested under several different test conditions. The data clearly shows that there are several important parameters which govern tire longitudinal stiffness behavior. At a minimum, inflation pressure, tread depth, normal loading and temperature have a strong influence on linear longitudinal stiffness estimates for low values of slip. Surprisingly, road lubrication by water had the smallest influence on longitudinal stiffness estimates of all test conditions

8 Future Work

Tire cornering stiffness exhibits different sensitivities to inflation pressure, tread depth and normal load than longitudinal stiffnesses [18]. It may be possible to combine sideslip [17, 10] and longitudinal slip estimators, possibly with a Bayesian network [19], such that inflation pressure and tread wear may be reliably inferred. Additionally with the recent advances toward in-tire temperature and pressure sensors, it may be possible to further isolate tread temperature and inflation pressure effects from other operating conditions.

There are several details remaining for a practical real time implementation of a longitudinal stiffness estimator of this form. Recent work in [1] demonstrates real time mass, road grade, rolling resistance and aerodynamic drag estimation. These proposed schemes would allow slip estimation under more realistic driving conditions. Furthermore brake force modeling, pitch dynamics and incorporation of the GPS sensor into the estimation scheme will allow for slip testing under braking and on 4 wheel drive vehicles.

There appears to be little information about wet verses dry roads embedded in tire behavior for low values of slip, however, these tests were far from exhaustive. Future work will experiment with lower peak friction surfaces and identify how far outside of the linear region the influence of road surface becomes more apparent.

9 Acknowledgements

The authors would like to thank Dr. Skip Fletcher, T.J. Forsyth, Geary Tiffany and Dave Brown at the NASA Ames Research Center for the use of Moffett Federal Airfield. The authors would also like to acknowledge Thomas Forchert and Dr. Bernard Baeker at DaimlerChrysler for donating the DaimlerChrysler-Stanford Research Vehicle. We also thank Mr. Karl Perras of DaimlerChrysler for donating the tires for this work.

References

[1] H. S. Bae, J. Ryu, and J. C. Gerdes. Road Grade and Vehicle Parameter Estimation for Longitudinal Control Using GPS. In *IEEE Conference on Intelligent Transportation Systems, Proceedings, ITSC*, pages 166–171, 2001.

[2] E. Bakker, L. Nyborg, and H.B. Pacejka. Tyre Modelling for Use in Vehicle Dynamics Studies. In *SAE Paper 870421*, 1987.

[3] Ake Bjorck. *Matrix Computations, 3^{rd} edition*. Society for Industrial and Applied Mathematics, Philadelphia, 1996.

[4] Carlos Canudas-De-Wit and Roberto Horowitz. Observers for Tire/Road Contact Friction Using Only Wheel Angular Velocity Information. In *Proceedings of the 38^{th} Conference on Decision and Control*, pages 3932–3937, 1999.

[5] Christopher Robert Carlson and J. Christian Gerdes. Identifying Tire Pressure Variation by Nonlinear Estimation of Longitudinal Stiffness and Effective Radius. In *Proceedings of AVEC 2002 6^{th} International Symposium of Advanced Vehicle Control*, 2002.

[6] David Bevly et al. The Use of GPS Based Velocity Measurements for Improved Vehicle State Estimation. In *Proceedings of the American Control Conference, Chicago IL*, pages 2538–2542, 2000.

[7] Gean H. Golub and Charles F. Van Loan. *Matrix Computatons, 3^{rd} edition*. The Johns Hopkins University Press, Baltimore and London, 1996.

[8] Fredrik Gustafsson. Slip-Based Estimation of Tire - Road Friction. *Automatica*, 33(6):1087–1099, 1997.

[9] Fredrik Gustafsson. Monitoring Tire-Road Friction Using The Wheel Slip. In *IEEE Control Systems Magazine*, pages 42–49, 1998.

[10] Jin-Oh Hahn and Rajesh Rajamani. GPS-Based Real-Time Identification of TireRoad Friction Coefficient. *IEEE Transactions on Control System Technology*, 10, NO.3:331–343, MAY 2002.

[11] S. Van Huffel and Joos Vandewalle. *The Total Least Squares Problem:Compulational Aspects and Analysis*. Society for Industrial and Applied Mathematics, Philadelphia, 1991.

[12] Wookug Hwang and Byung-Suk Song. Road Condition Monitoring System Using Tire-Road Friction Estimation. In *Proceedings of AVEC 2000 5^{th} International Symposium of Advanced Vehicle Control*, pages 84–89, 2000.

[13] L. Ljung. *System Identification: Theory for the User*. Prentice-Hall, Inc., Upper Saddle River, New Jersey, 1999.

[14] Shannon L. Miller, Brett Youngberg, Alex Millie, Patrick Schweizer, and J. Christian Gerdes. Calculating Longitudinal Wheel Slip and Tire Parameters Using GPS Velocity. In *Proceedings of the American Control Conference*, 2001.

[15] Laura Ray. Nonlinear Tire Force Estimation and Road Friction Identification, Simulation and Experiments. *Automatica*, 33, no. 10:1819–1833, 1997.

[16] E.J. Rossetter and J.C. Gerdes. The Role of Handling Characteristics in Driver Assistance Systems with Environmental Interaction. In *Proceedings of the 2000 ACC, Chicago, IL*, 2000.

[17] Jihan Ryu, Eric J. Rossetter, and J. Christian Gerdes. Vehicle Sideslip and Roll Parameter Estimation Using GPS. In *Proceedings of AVEC 2002 6^{th} International Symposium of Advanced Vehicle Control*, 2002.

[18] H. Sakai. Theoretical and Experimental Studies on the Dynamic Properties of Tyres, part 4. *International Journal of Vehicle Design*, 3:333–375, 1982.

[19] M. L. Schwall and J. C. Gerdes. Multi-Modal Diagnostics for Vehicle Fault Detection: DSC-24600. In *Proceedings of IMECE 2001*, 2001.

[20] H. Schwetlick and C. Tiller. Numerical Methods for Estimating Parameters in Nonlinear Models With Errors in the Variables. *Technometrics*, 27(1):17–24, 1985.

[21] Michael Uchanski. *Road Friction Estimation for Automobiles Using Digital Signal Processing Methods*. PhD thesis, University of California, Berkeley, Fall 2001.

[22] A. T. van Zanten. Evolution of Electronic Control Systems for Improving the Vehicle Dynamic Behavior. In *Proceedings of the 6^{th} International Symposium on Advanced Vehicle Control*, 2002.

[23] Kyongsu Yi, Karl Hedrick, and Seong-Chul Lee. Estimation of Tire-Road Friction Using Observer Based Identifiers. *Vehicle System Dynamics*, 31:233–261, 1999.